Exploring the link between interfacial and bulk viscoelasticity in reverse Pickering emulsions

Santiago Velandia, Diego Ramos, Maud Lebrun, Philippe Marchal, Cécile Lemaitre, Véronique Sadtler, Thibault Roques-Carmes

Exploring the link between interfacial and bulk viscoelasticity in reverse Pickering emulsions

Santiago F. Velandia, Diego Ramos, Maud Lebrun, Philippe Marchal, Cécile Lemaitre, Véronique Sadtler, Thibault Roques-Carmes*

Laboratoire Réactions et Génie des Procédés, UMR 7274 CNRS, Université de Lorraine, 1 rue Grandville, 54001 Nancy, France

(*) corresponding author: Thibault Roques-Carmes: thibault.roques-carmes@univ-lorraine.fr, Tel.: +33 (0)3 72 74 38 33

Abstract

The relationship between interfacial and bulk emulsion viscoelasticity is investigated. Water-in-dodecane reverse Pickering emulsions, with a dispersed phase volume fraction of 0.66, stabilized with partially hydrophobic silica particles are addressed. Interfacial and bulk viscoelastic properties are probed *via* 2D and 3D oscillatory shear rheology. The silica particles concentration and NaCl content have been varied. In the whole range of concentrations studied the elastic modulus (G') remains always greater than the viscous modulus for 2D and 3D rheology. The viscoelastic behavior can be related to the silica concentration both at the interface and in the emulsion. Power law dependences towards the silica content are recorded for the interfacial and the bulk emulsion elastic modulus. When increasing the NaCl concentration, the viscoelastic properties both at the interface and in the emulsion become stronger. The amount of silica and NaCl produces similar effects on both the interface and bulk viscoelastic properties. The increase of their concentration induces a rigidification of the dodecane/water interface since G_P'(interface) increases. Such interfacial hardening produces a rigidification of the droplets (G_P'(Emulsion) is enhanced). Correlations between the interfacial and bulk emulsion viscoelasticity are also extracted from the experimental data. This is the first time that these kinds of relationship are reported. These results highlight that everything that affects the interfacial viscoelasticity is reflected on the bulk scale of emulsions.

KEYWORDS Pickering; W/O Emulsions; Interfacial Rheology; Bulk Rheology; Nanoparticles

1) Introduction

Particle stabilized emulsions, otherwise known as Pickering emulsions, are claimed to be highly stable against coalescence [1,2]. As a consequence, this behaviour has not only drawn the scientists' attention but it has also promoted the developement of new products [3-5]. Pickering emulsions appear also as an interesting alternative in comparison to the classic surfactant stabilized emulsions. Many studies have previouly shown that the behavior of these dispersed systems depends mainly on the distribution of the particles in the continuous phase and, especially, at the oil/water interfaces of the droplets [6-8].

To probe the interfacial properties, interfacial rheology appears as a useful tool [9,10]. Several techniques are available to study the rheological behavior at interfaces. They can be divided into two groups depending on the mode of deformation of the interface, namely shear and dilation [9-11]. On the one hand, interfacial dilatational rheometry includes mainly drop shape tensiometry and through methods based on the Langmuir film balance [11,12]. The latter is well suited to investigate the dilatational properties of the interface by moving a barrier on a planar fluid interface that can be used to compress or dilate the interface [13,14]. This method is generally used to determinate the particle amount at the interface when equilibrium is reached. While some approaches have been developed to use the Langmuir trough with O/W interfaces, these measurements still require some modification of the current apparatus [15]. The most popular systems for dilatational/compressional rheometry remain those based on the drop shape tensiometry [9-11]. The measurements are based on the interfacial tension studies to follow the relaxation of interfacial layers (droplets) after respective harmonic or transient perturbations [9-11]. On the other hand, interfacial rheometry

can be probed by direct shearing of interfaces. For this purpose, special biconical and double wall ring geometries are connected to classical rotational rheometer [16-18].

Several attempts have been made to find relationships between interfacial phenomena and emulsions stability. The interfacial rheology appears as a relevant method to explain coalescence, flocculation and even Ostwald ripening [19-23]. Only recently, authors have been interested to find a link between interfacial and bulk emulsion rheology properties. Only three studies compared interfacial *versus* bulk rheology for Pickering emulsions [24-26]. Dockx et al. have developed a very relevant strategy in order to obtain a direct relation between the emulsion stability and the interfacial rheology [24]. More recently, comparison of the interfacial viscoelasticity with the bulk emulsion viscoelasticity was introduced by Kamkar et al. for emulsions stabilized with silica nanoparticles and polymers [25]. The main aim was to discuss the localization of the nanoparticles in oil, water and at the interface. However, the objective was mostly to emphasize that the interfacial rheology dominates oil/water stabilization over bulk emulsion rheology. The study focused on the relationship between the interfacial rheological properties and the stability of the emulsion against coalescence. It was demonstrated that emulsion stability can be linked to a strong viscoelastic film of particles at the oil/water interface. The high stability came from the solid-like property of the interface, quantified by high values of the interfacial elastic modulus.

Thus, the present-day ability to find relationships between the viscoelastic properties of the emulsion in the whole volume and the interfacial viscoelastic rheological properties is still significantly restricted. There is a need for more experimental data so that one of the aims of this article is to provide additional ones. The emulsification process is generally conducted with homogenizer which shear the oil/water interfaces. Rotor-stator disperser and Rushton turbine are some examples. Consequently, it appears that drop shape tensiometry based on dilatation/compression of the droplets does not fully represent the system during the droplet

formation but is more adapted to understand the droplets stability against coalescence, flocculation and Ostwald ripening [20-23]. Conversely, shear interfacial rheology (with bicone or double wall ring systems) seems more pertinent to represent the shear forces to which the interfaces are subjected during the emulsification process. In addition, the system seems closer to the rheology of the whole emulsion in volume (plate-plate geometry for instance) since both are shear rheometry. To ensure a better measurement sensitivity of interfacial shear rheology, oscillatory tests (viscoelasticity of the interface) have to be performed rather than flow experiments (viscosity). It becomes then possible to attempt to build a relationship between the viscoelastic properties of the emulsion in the whole volume and the interfacial viscoelastic rheological properties. This is carried out here for reverse water-in-dodecane Pickering emulsions with a dispersed phase volume fraction of 0.66 stabilized with partially hydrophobic silica particles and emulsified by the means of an Ultra-turrax® homogenizer. The interfacial shear rheology experiments are performed with a stress-controlled rheometer coupled with double wall ring (DWR) geometry.

2) Materials and methods

2.1) Chemicals and phases preparation

Dodecane was obtained from ReagentPlus® (purity ≥ 99%). Aerosil® R-972 was used as stabilizing particles (provided by Evonik). These nanosized fumed silica particles (diameter of 16 nm) were methylated with dimethyl chlorosilane to reach 70% of surface hydrophobization.

The aqueous and oily phases were prepared separately following the same protocol for both applications (interfacial rheology and emulsions). The oily phase was a dispersion of silica in dodecane. The silica was dispersed in the dodecane oil by the means of ultrasounds generated by a Sonic Dismembrator 550 (Fisher Scientific-20 kHz frequency-standard probe).

The suspension was sonicated during 90 s by alternating ultrasound pulse of 2 s and absence of pulse of 2 s at a fixed amplitude of 70%. The increase of temperature was mitigated with an ice bath placed under the beaker. For interfacial rheology measurements, the silica concentration was given relatively to the mass of oil, and was varied between 0.001 and 10 wt.%. For emulsion and bulk rheology, the silica content was reported relatively to the total amount of water dispersed phase in the W/O emulsion, and was varied between 0.5 and 2 wt.%. The water phase consisted of de-ionized water unless stated otherwise. In some cases, sodium chloride was dissolved inside the water (part 3.2). For the two applications (interface and emulsion), the NaCl content was given relatively to the mass of water.

2.2) Interfacial rheology

Interfacial shear rheology experiments were conducted with a stress-controlled AR-G2 rheometer and a double wall ring geometry (DWR), both from TA Instruments. Such geometry consisted of a diamond-edged ring made of Pt/Ir and a holding trough made of Teflon. A picture of the system is provided in Fig. S1a of the Supporting Information. The most crucial step in using DWR is to ensure the proper placement of the ring at the interface of the two liquids. In order to overcome this complicated step, the following procedure was adopted. First, the water phase was added into the cylindrical reservoir until the middle edge of the cell. Then, the head of the rheometer was lowered until the ring was near the liquid surface (approximately 12 mm, see Fig. S1b of the Supporting Information). The speed of the head was reduced and lowered until it just touched the interface of water. At that time, the computer was used to lower 500 µm of the head, i.e. one half of the height of the ring so that the edge of the ring was positioned at the oil/water interface (Fig. S1c of the Supporting Information). In parallel, the oil phase containing the particles was redispersed using ultrasounds just before the interfacial rheometry experiment. The oil phase containing the

particles was gently added with a syringe over the ring and water phase. The volume of oil was fixed to 5 mL. To study the interfacial viscoelasticity, small amplitude oscillating stress sweep experiments were applied. A sinusoidal shear stress was applied to the interface at an angular frequency of 1 rad/s. In our experiments, the oscillatory interfacial stress was varied between 10^{-6} and 10^{-1} N/m. The stress was low enough to maintain the structure of the interface at the beginning of the test, but while the test progressed, the increase of stress could cause the destruction of the structure and lead to the drop of elastic modulus and viscous modulus. A shear stress of 10^{-1} N/m might be too high but this aspect will be discussed in the next paragraph. The elastic/storage modulus G'(interface) and loss/viscous modulus G''(interface) were obtained from these experiments. At minimum, each experiment was performed in duplicate to assess reproducibility. The reported results correspond to the average between repetitions. Data were considered acceptable only if the results between replicates differ by less than 10%. The temperature was maintained at 25 °C during the experiment.

Several parameters can be obtained from the results based on the evolution of the interfacial viscoelastic modulus as a function of the oscillatory stress and strain. An example of typical curves is reported in Figure 1. They are representative of nearly all the interfacial rheological results. The data are displayed for stresses between 10^{-6} and 10^{-1} N/m which correspond to strains ranging from 10^{-6} to 10^{3}. For shear strains larger than 10^{-1}, the deformation becomes large enough to induce a disorganization of the interface so that the results will not be discussed in this zone. It was decided to maintain the plot of the data in the whole domain in order not to miss information. However, the results were not considered and discussed at high shear stresses and strains where all the points collapse to a single value (G'(interface) = 10^{-6} N/m) regardless of the systems. This reasoning is maintained in all cases (silica content (Fig. 2) and salt concentration (Fig. S6 of the Supporting information)). The

G'(interface) remained constant at low shear strain (γ) and shear stress (τ) in the linear viscoelastic regime while it decreased at larger γ and τ. Furthermore, linear viscoelastic regions characterized by the G' "plateau" were observed in each diagram. The value extracted from this zone was denoted G_P'(interface). Stress and strain amplitude sweeps allowed identifying the yield stress and strain, τ_Y(interface) and γ_Y(interface), respectively. They represented the conditions of particles network breakage at the interface and provided insight into the intensity (via τ_Y) and extent (via γ_Y) of interactions at the interface. A tangent method was used to determine τ_Y(interface) and γ_Y(interface) by defining them as the crossing point between the tangents from the linear viscoelastic region and the tangent from the decreasing part of the curve. Fig. 1 gives an example of the methodology. Note that the approach currently used in volumetric rheology with emulsions was applied to interfacial rheology since it has been illustrated in several reports as the more robust and accurate method to estimate the yield stress [27]. Additionally, γ_{LD}(interface) and τ_{LD}(interface) were denoted as the boundary conditions of the linear viscoelastic region under which the network of particles at the interfaces begin to break or at least to respond non-linearly to mechanical strains or stresses. These conditions were defined by taking the values of γ and τ for which the G'(interface) differed by 20% from that of G_P'(interface).

It is now well established that the anchoring of the particles at the interface takes some time [28]. To ensure that the rheological properties were measured in the presence of the exact amount of particles that corresponded to the equilibrium, the following approach was used. The rheological properties (interface elastic and viscous modulus) were measured at different times while maintaining all the system conditions unchanged. It was considered that the system reached steady state when the G'(interface) and G''(interface) values did not vary between the experiments conducted at different times. These values had to stay constant during 2-3 hours. The last oscillatory strain sweeps (interfacial G' as a function of shear strain

and shear stress) was reported in the figures of the paper. The time to reach equilibrium depended on the particle content.

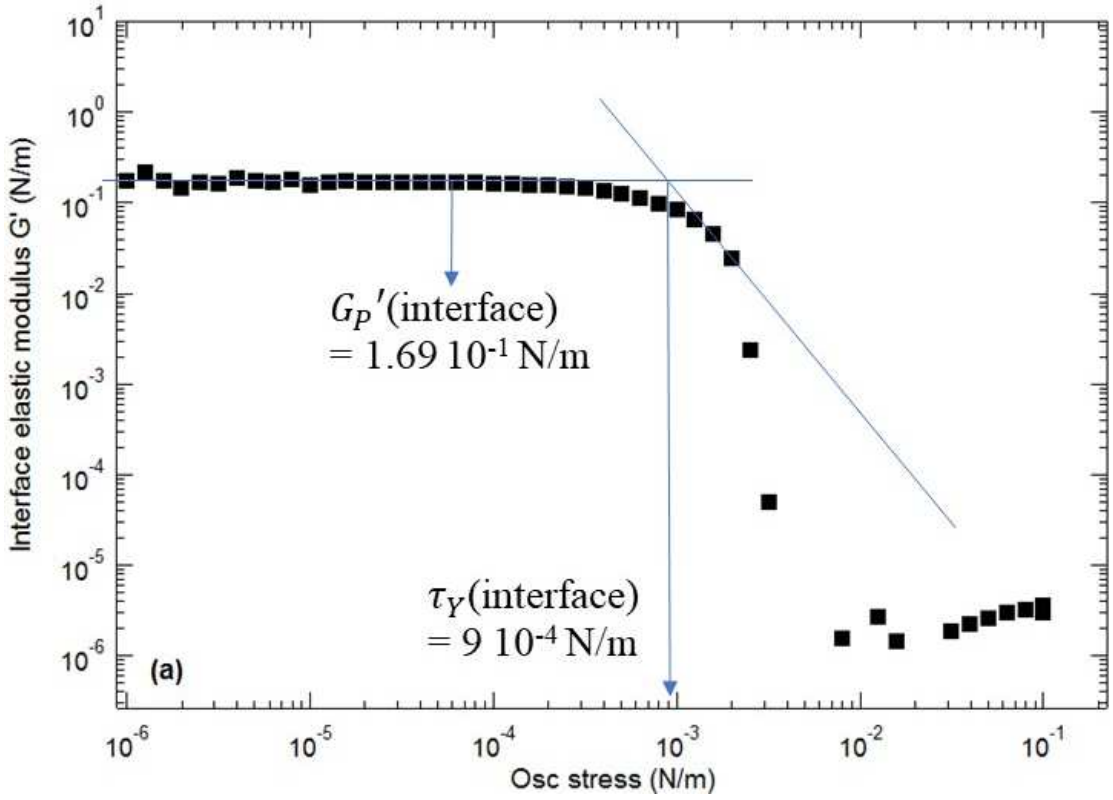

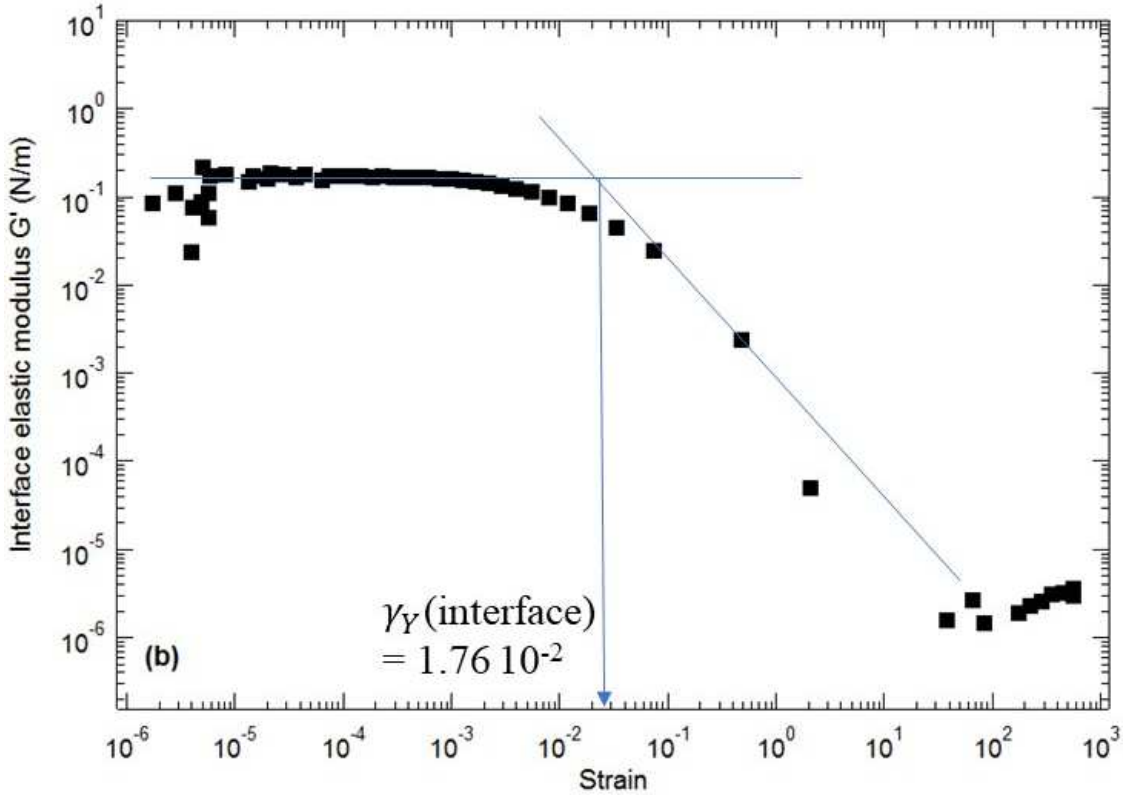

Figure 1. Methodology used to determine graphically the yield stress τ_Y(interface) and strain γ_Y(interface) as well as the elastic modulus value in the linear viscoelastic domain G_P'(interface) of the dodecane/water interface.

2.3) Emulsion preparation and bulk rheology

The preparation of the Pickering reverse emulsions was performed using the following protocol. The aqueous phase was added to the oil phase containing the silica particles at a 5.2 mL min^{-1} flow rate by means of a peristaltic pump (BVP-Ismatec). This process was conducted under agitation with an Ultra-Turrax® homogenizer (IKA T25 Basic / Dispersion Tool S25-NK-19G, Germany) at a rate of 13500 rpm. At the end of this stage, the emulsion homogenization was performed for 3 min by moving the head of the rotor-stator from bottom to top to counteract local dead zones during the whole agitation process.

For all the emulsions, the water dispersed phase volume fraction was fixed to 0.66. Note that this value is close to the random close packing volume fraction of monodisperse spheres (0.64). It was then considered that the droplets had already percolated, due to the volume fraction of droplets and particles involved in this study. The space between the droplets was small and it was expected that the relationships between the interfacial and volumetric properties were more sensitive for percolated systems than for diluted emulsions.

As preliminary tests, dilution in water and dodecane, conductivity and droplet size distribution were evaluated. The droplet size distribution was determined by means of optical microscopy coupled to image processing. A minimum of 400 droplets were used to obtain a reliable droplet size distribution.

An ARES rheometer from TA instruments was used to evaluate the rheology of emulsions. The measurements were performed with a parallel plates geometry (25 mm of diameter and a gap of 1 mm) and maintaining a temperature of 20 °C. Prior the rheological measurements, the emulsions were gently and manually stirred in order to ensure the homogeneity of the

samples while maintaining their structure. The oscillatory tests were conducted in order to evaluate the structural properties of the emulsions. To this aim, oscillatory strain sweeps were performed by increasing shear strain from 10^{-4} to 1 while maintaining the frequency to 1 rad/s. From the tests, the viscoelastic characteristics (G', G'') of the emulsions can be obtained for various shear strains and shear stresses. The methodology used to determine graphically the elastic modulus value in the linear viscoelastic domain G_P'(Emulsion), the yield stress τ_Y(Emulsion) and strain γ_Y(Emulsion) from the oscillatory strain sweeps curves (G' vs shear strain and shear stress) is depicted in the Fig. S2 of the Supporting information. Note also that γ_{LD}(Emulsion) and τ_{LD}(Emulsion) were obtained by reporting the values of γ and τ for which G'(Emulsion) varied by 20% from that of G_P'(Emulsion). Duplicate measurements were performed for each sample to ensure repeatability of the rheological data.

The stability of emulsions was assessed by comparing their rheology just after preparation (0 days) and after 15 days of storage. Samples were stored under constant conditions of temperature and pressure (20 ºC, 1 atm).

3) Results and discussion

3.1) Effect of silica content

3.1.1) Interfacial rheology

The influence of the silica content on the evolution of the interfacial elastic modulus (dodecane/water interface) as a function of the oscillatory stress and strain is displayed in Figure 2. For all the silica contents, the elastic modulus G' remains larger than the viscous modulus G'' (Fig. S3 of the Supporting information). This highlights an elastic behavior of the dodecane/water interface in presence of silica particles at the interface. In the following, only the evolution of the extracted interface elastic modulus in the linear viscoelastic regime G_P'(interface), the interface yield stress τ_Y(interface) and the interface yield strain

γ_{LD}(interface) with the silica content are discussed and reproduced in the Figure 3 and Table 1.

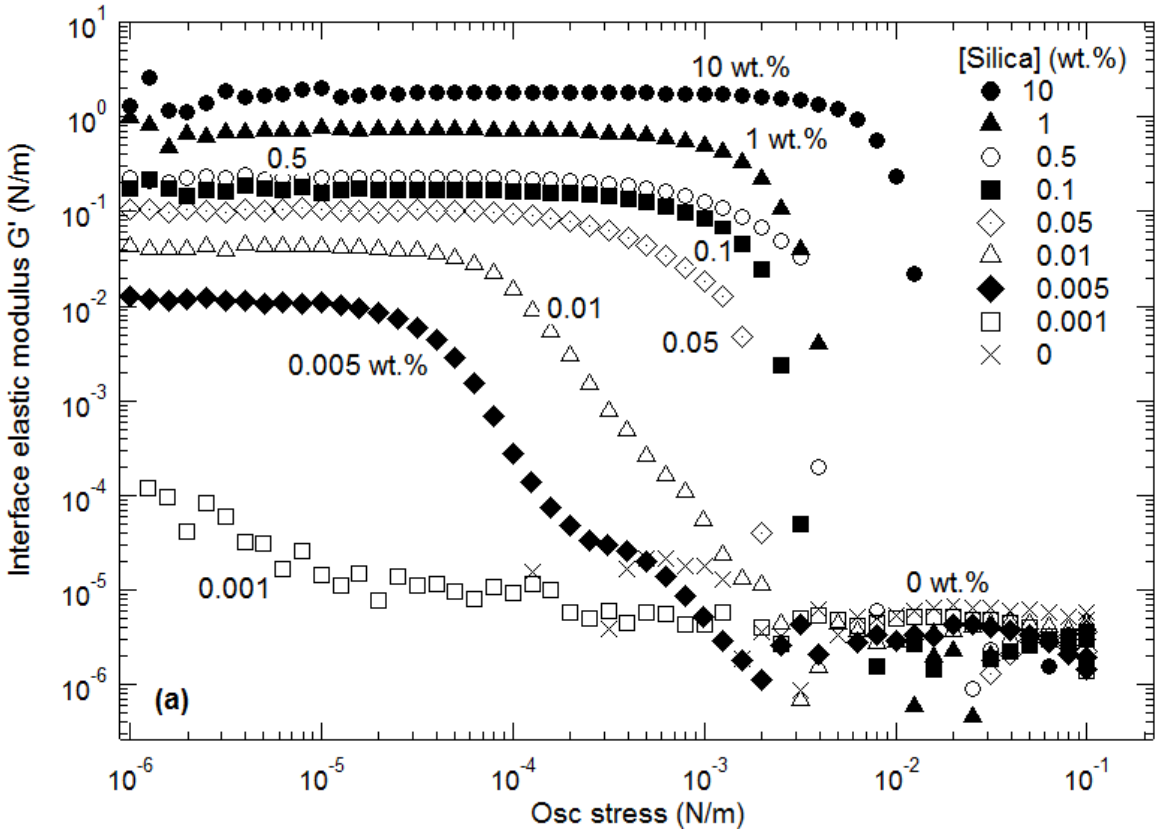

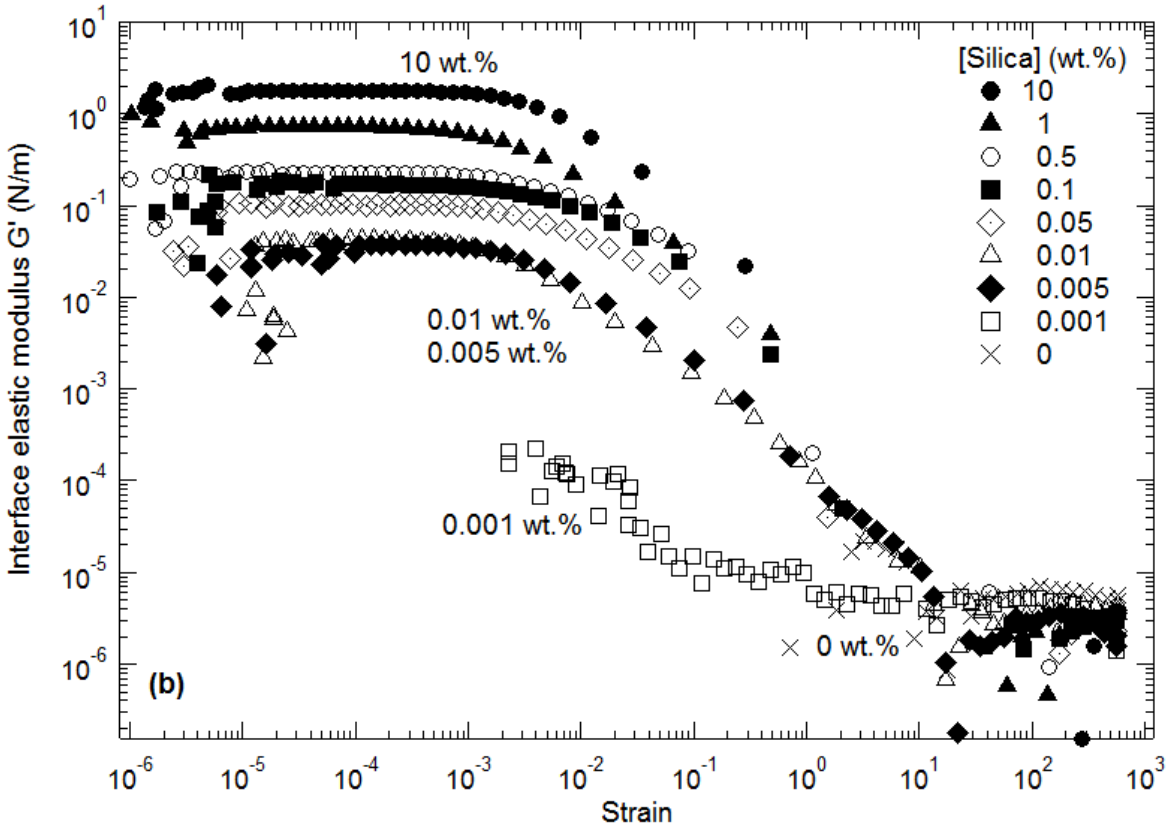

Figure 2. Variation of the interface elastic modulus as a function of the (a) oscillatory stress, and (b) strain for various silica contents. [NaCl] = 0 wt.%.

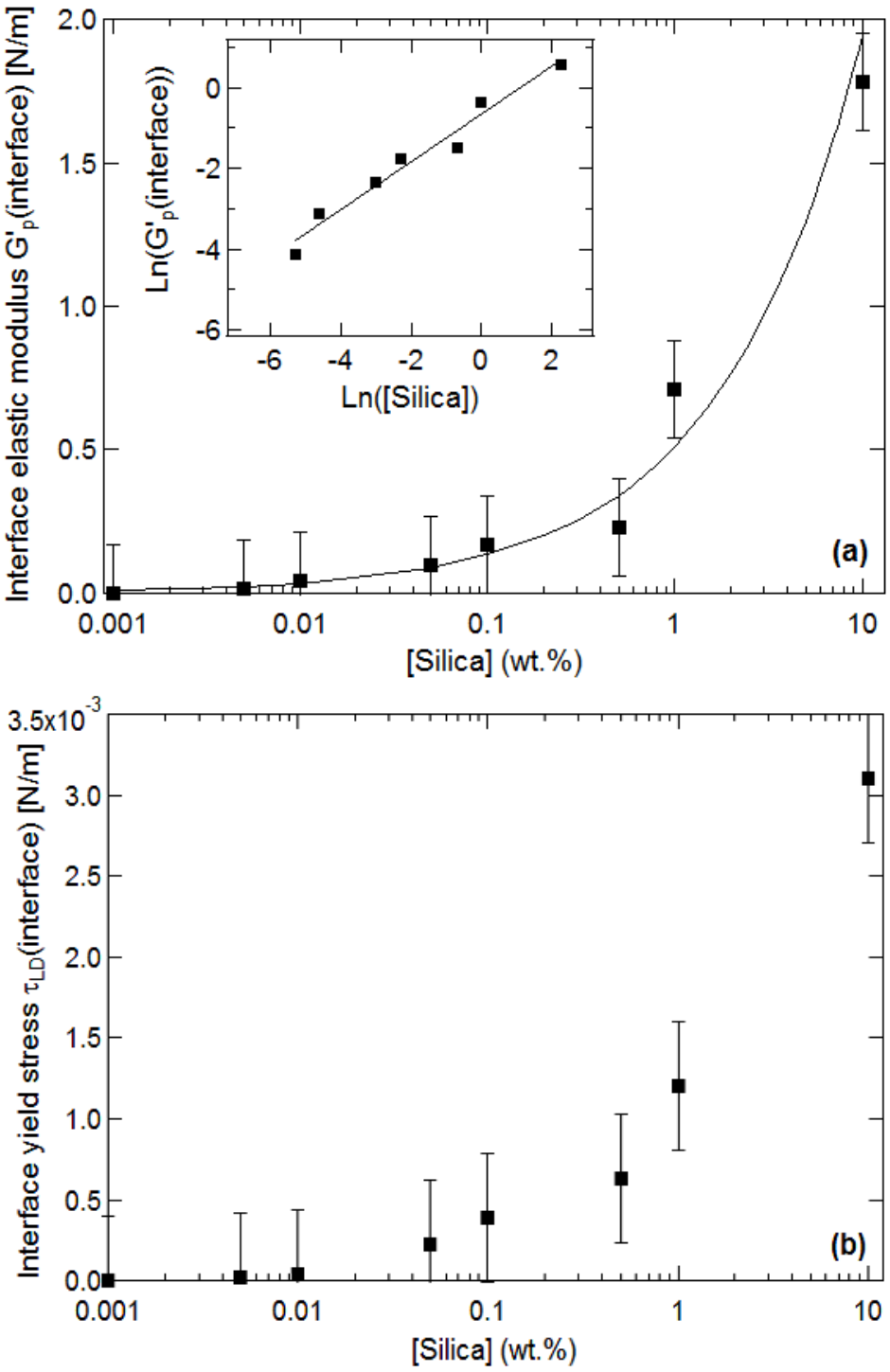

Figure 3. Evolution of the (a) interface elastic modulus G_P'(interface), and (b) interface yield stress τ_Y(interface) with the silica content [Silica]. The points correspond to the experimental data while the line represents the best fit given by G_P'(interface) = 0.51 [Silica]$^{0.58}$ (R^2 = 0.9653). [NaCl] = 0 wt.%. Inset: Ln(G_P'(interface)) plotted against Ln([Silica]). The line represents the best linear fit.

In the absence of silica and in the presence of 0.001 wt.% of silica in oil, the interface elastic modulus G_P'(interface) appears relatively low, around 10^{-5}-10^{-4} N/m (Fig. 3a). These kinds of values were already obtained by Reynaert et al. for 0.1 µm polystyrene soft particles [28]. At larger silica content, *i.e.* larger than or equal to 0.005 wt.%, G_P'(interface) increases considerably reaching values between 10^{-3} and 1.75 N/m. Note that these data are in the same order of magnitudes than those reported by Kamkar et al. and Lin et al. [25,29]. It was reported that the interfacial elastic modulus of water/silicone oil increased from 10^{-1} to 5 10^{-1} N/m when the silica content increased from 1 to 4 wt.% [25]. Values between 10^{-1} and 1 N/m were recorded for asphaltene at air/water and decane/water interfaces [29].

It appears also that G_P'(interface) increases with the silica content (Fig. 3a). More particularly, G_P'(interface) follows a power law dependence with the silica content of the form G_P'(interface) = 0.51 [Silica]$^{0.58}$ (Fig. 3a inset). This kind of scaling law has already been reported at the liquid/liquid, liquid/air interfaces and also in the bulk [28-30]. This power law evolution indicates that a 2-dimensional aggregate structure, generally a fractal network, similar to a gel takes place at the interface [28-30]. The model, based on the scaling law, is supported by the existence of the elastic links between aggregates. The structure of the interfacial network can be deduced from the equation

$$G_P'(\text{interface}) \sim \Theta^n = \Theta^{\frac{d + D_{bh}}{d - D_f}} \qquad (1)$$

where Θ is the silica phase volume fraction, n the power law exponent, d the dimension of the Euclidean space, D_f the fractal dimension of the aggregate network, and D_{bh} the fractal dimension of the backbone of the network [28].

To use this model in the present study, the G_P'(interface) values were replotted against Θ instead of the silica weight fraction. When the data are fitted by a power law of the form of equation (1), the power law index n reaches a value of 0.59. Exponents of 2-11 are generally encountered for particles at the liquid/liquid interfaces. For example, a power law exponent of

8 for polystyrene particles at the water/decane interface was obtained [28]. Power law exponents ranging between 5 and 11 were reported for asphaltene at the decane/water interface for various shear rates and depending on chemical dispersants added (alkyl phenol or octyl phenol) [29]. The value of the power law exponent recorded in the present study appears then much lower than the values depicted in the literature. The larger values reported by other authors can be explained by a difference in particle's nature, size, and morphology (micrometric sulfate polystyrene particles [28] and asphaltenes [29]).

The impact of the silica concentration on the interfacial yield stress and strain can be also discussed (Fig. 3b and Table 1). The yield stress τ_Y(interface) and linearity limit τ_{LD}(interface) both increase with the silica content. This emphasizes that the breakage of the silica network at the dodecane/water interface requires a much higher stress intensity when the silica amount is enhanced. Conversely, the yield strain γ_Y(interface) as well as the linearity limit γ_{LD}(interface) do not vary monotonically with the silica content. Data are distributed around an average value of 5.1×10^{-3}. This trend is confirmed in the Figure 2b where the interfacial elastic modulus is plotted as a function of the oscillatory strain for various silica contents. In fact, it was considered that there is no difference in yield strain regardless of the silica content. This highlights that the extent of the interaction between the particles at the interface is not modified by the silica content. This result was expected since the interaction strength can be only affected by a change of oil, pH, ionic strength, surfactant or addition of other additives [9,10].

Table 1. Linear viscoelastic limits (γ_{LD}(interface) ; τ_{LD}(interface)) and threshold values (γ_{Y}(interface) ; τ_{Y}(interface)) as a function of silica concentration obtained from Fig. 2a-top (G'(interface) vs. shear stress $\tau \rightarrow \tau_Y$(interface) ; τ_{LD}(interface)) and Fig. 2b-bottom (G'(interface) vs. shear strain $\gamma \rightarrow \gamma_Y$(interface) ; γ_{LD}(interface)).

[Silica] (wt.%)	$G_P{}'$(interface) [N/m]	τ_Y(interface) [N/m]	τ_{LD}(interface) [N/m]	γ_Y(interface)	γ_{LD}(interface)
0	8.0×10^{-6}				
0.001	1.3×10^{-4}	9.9×10^{-7}	1.2×10^{-6}		
0.005	1.6×10^{-2}	1.6×10^{-5}	4.0×10^{-5}	5.0×10^{-3}	8.0×10^{-3}
0.01	4.4×10^{-2}	3.9×10^{-5}	7.0×10^{-5}	2.5×10^{-3}	1.1×10^{-3}
0.05	9.7×10^{-2}	2.2×10^{-4}	5.0×10^{-4}	1.7×10^{-2}	2.5×10^{-3}
0.1	1.7×10^{-1}	3.9×10^{-4}	9.0×10^{-4}	1.7×10^{-2}	2.2×10^{-3}
0.5	2.3×10^{-1}	6.3×10^{-4}	1.1×10^{-3}	4.0×10^{-3}	2.1×10^{-3}
1	7.9×10^{-1}	1.2×10^{-3}	2.6×10^{-3}	2.0×10^{-3}	8.5×10^{-4}
10	1.78	3.1×10^{-3}	7.4×10^{-3}	3.0×10^{-3}	2.9×10^{-3}

3.1.2) Emulsion rheology

All the formulated Pickering emulsions present the ability to be diluted in dodecane. Conductivity values lower than 10^{-5} S cm^{-1} are obtained. This confirms the presence of reverse emulsions regardless of the silica content. Fig. S4 of the Supporting information presents droplet size distributions after varying silica particle concentration. All the prepared emulsions are polydisperse but monomodal with droplet sizes ranging from 10 to 60 µm. However, a narrowing of the droplet size distribution can be noticed with the increase of the particle content. In other words, the narrower size distribution was recorded for a particle concentration of 2 wt.%. The calculated mean droplet size of the emulsions are equal to 28 µm, 26 µm, and 20 µm for emulsions prepared with 0.5, 1 and 2 wt.% of silica, respectively.

For all the prepared emulsions, the storage modulus *G'* is larger than the loss modulus *G''* regardless of the silica concentration. This indicates the predominance of the solid-like/elastic behavior of the emulsions in the range of concentrations considered here. The effect of particle concentration on *G'* modulus is presented in Fig. S5 of the Supporting information ("0

days"). The extracted G_P'(Emulsion), linearity limits, yield stress and strain values are reported in the Figure 4 and the Table 2 ("0 days"). Particle concentration has a major impact on the rheology of Pickering emulsions since the elastic modulus increases significantly with particle concentration (Figure 4a). This aspect has been already reported in the literature [31-32]. Indeed, the emulsions prepared at 1 wt.% of particle concentration present an increase of G_P'(Emulsion) of a factor 2.4 with respect to systems at 0.5 wt.%. In the same vein, the 2% by weight formulation shows an increase in elastic modulus by a factor 2 compared to 1 wt.% formulation. In other words, G_P'(Emulsion) values are between five and six times higher than those of emulsions at the lower particle concentration. It is important to note that for all 3 formulations, the silica content, *i.e.* the mass of particles, is larger than that theoretically expected for a monolayer ensuring the maximum geometric coverage of the droplets by the particles organized in a hexagonal structure given as 0.42 wt.% (detail of the calculation available in the Supporting information). This implies that in every formulation case, the system is "overloaded" with nanoparticles. As the dispersed phase volume fraction remains constant, G_P'(Emulsion) variation is only attributed to particle organization in the emulsions.

In addition, the data can be represented by a power law of the form G_P'(Emulsion) = 1350 [Silica]$^{1.16}$ (R^2 = 0.9945). This kind of evolution is representative of a gel behavior of the emulsions [30,33]. In parallel, the emulsion yield stress increases also with the silica content (Fig. 4b). This indicates that larger stresses are necessary to produce the breakage of the emulsion as the silica amount is enhanced. No significant variation of the yield strain can be observed (Table 2) indicating that the spatial range of the interactions between the particle/droplets are similar regardless of the silica content.

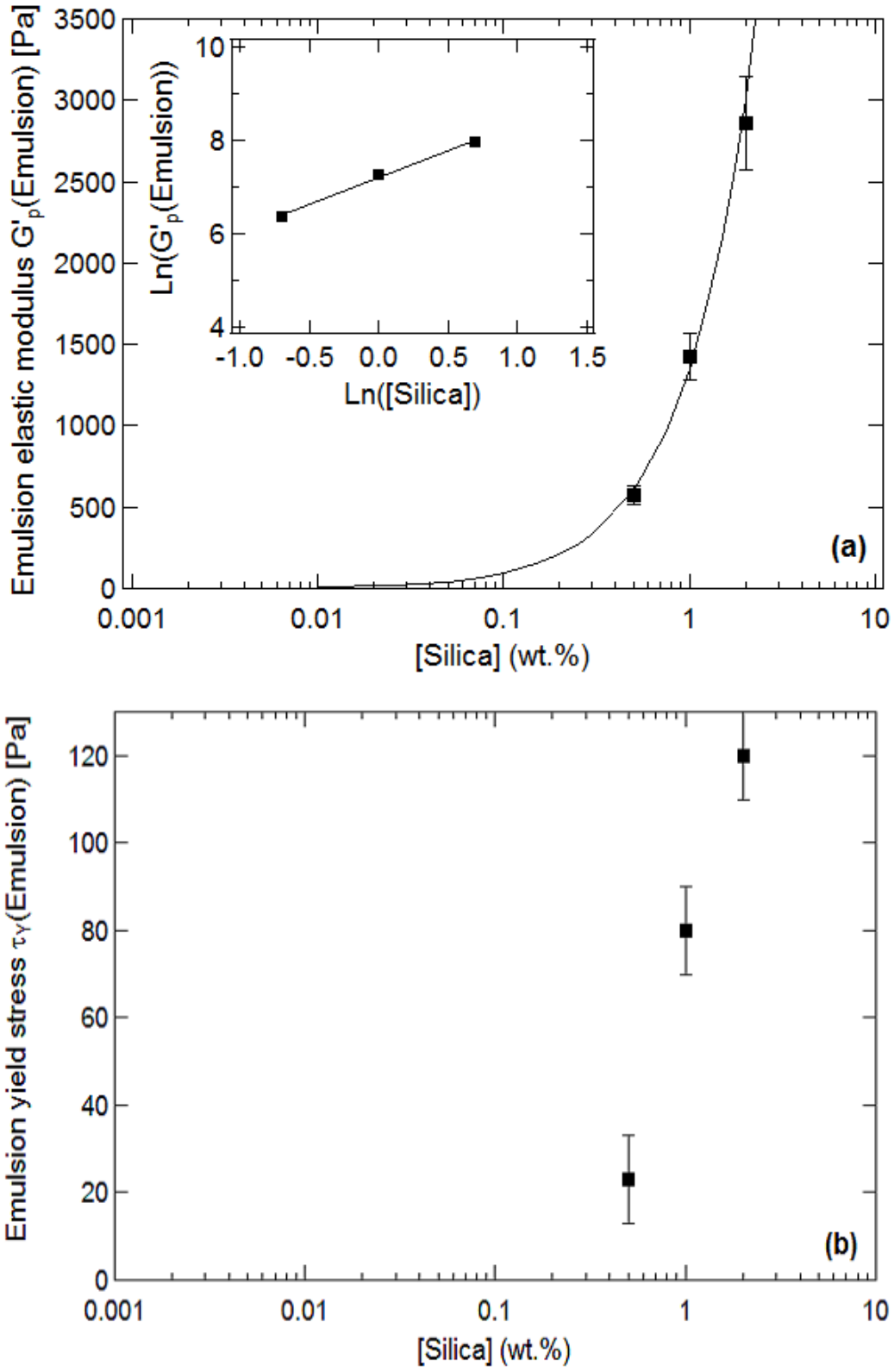

Figure 4. Evolution of the (a) emulsion elastic modulus G_P'(Emulsion), and (b) emulsion yield stress τ_Y(Emulsion) with the silica content [Silica]. The points correspond to the experimental data while the line represents the best fit given by the relation G_P'(Emulsion) = 1350 [Silica]$^{1.16}$ (R^2 = 0.9945). Inset: Ln(G_P'(Emulsion)) plotted against Ln([Silica]). The line represents the best linear fit.

Table 2. Linearity viscoelastic limits (γ_{LD}(Emulsion) ; τ_{LD}(Emulsion)) and threshold values (γ_Y(Emulsion) ; τ_Y(Emulsion)) as a function of particle concentration obtained from Fig. S5-top (G'(Emulsion) vs. shear strain $\gamma \rightarrow \gamma_Y$(Emulsion) ; γ_{LD}(Emulsion)) and Fig. S5-bottom (G'(Emulsion) vs. shear stress $\tau \rightarrow \tau_Y$(Emulsion) ; τ_{LD}(Emulsion)).

[Silica] (wt.%)	G_P'(Emulsion) [Pa]	τ_Y(Emulsion) [Pa]	τ_{LD}(Emulsion) [Pa]	γ_Y(Emulsion)	γ_{LD}(Emulsion)
0.5 0 Days	574	23	8	0.070	0.020
1 0 Days	1421	80	27	0.095	0.032
2 0 Days	2861	120	51	0.070	0.032
0.5 15 Days	457	20	11	0.060	0.040
1 15 Days	1203	60	27	0.073	0.040
2 15 Days	2542	110	46	0.068	0.032

3.1.3) Interfacial vs bulk rheology

The comparison between the bulk and interfacial rheological properties is not straightforward even if the two systems follow the same trend. For both (bulk and interface), G_P' increases with the silica content. Furthermore, a power law dependence towards the silica content has been obtained for the interface and the emulsion. Similarly, the yield stress at the interface and in the bulk is enhanced as the silica content is increased. The yield strain remains unaffected by the amount of silica at the interface or in the emulsion. To refine the reasoning and compare safely the bulk and interfacial rheological properties, the following approach was used. Since the volume and interfacial G_P' have different units, the G_P' were normalized by their maximum value to unify the comparison, *i.e.* G_P'(interface)/G_P'(interface, 10 wt.% silica) and G_P'(Emulsion)/G_P'(Emulsion, 2 wt.% silica). The idea is to plot on the same figure the normalized G_P'(interface) and G_P'(Emulsion). Figure 5a represents the parallel evolution of the normalized G_P'(interface) and G_P'(Emulsion)

as a function of the silica uptake. The data are very close. Interestingly, the change of normalized elastic modulus from 0.5 to 1 wt.%. is similar for both systems. This indicates a relationship between the bulk and interfacial elastic modulus G_P'. The similarity between the results is very interesting. The increase of the silica content induces a rigidification of the dodecane/water interface as G_P'(interface) increases. In parallel, the rigidification of this interface produces a rigidification of the emulsion and droplets. These conclusions apply also for the normalized yield stresses (Figure 5b) despite a larger discrepancy between the bulk and interface data for the normalized yield stresses, *i.e.* τ_Y(interface)/τ_Y(interface, 10 wt.% silica) and τ_Y(Emulsion)/τ_Y(Emulsion, 2 wt.% silica). Actually, the graphical determination of the yield stresses suffers from non-neglectable uncertainties. As a consequence, it can be concluded that each parameter that affects the interface of the droplets (here the silica content) has an impact on the volumetric behavior of the emulsion.

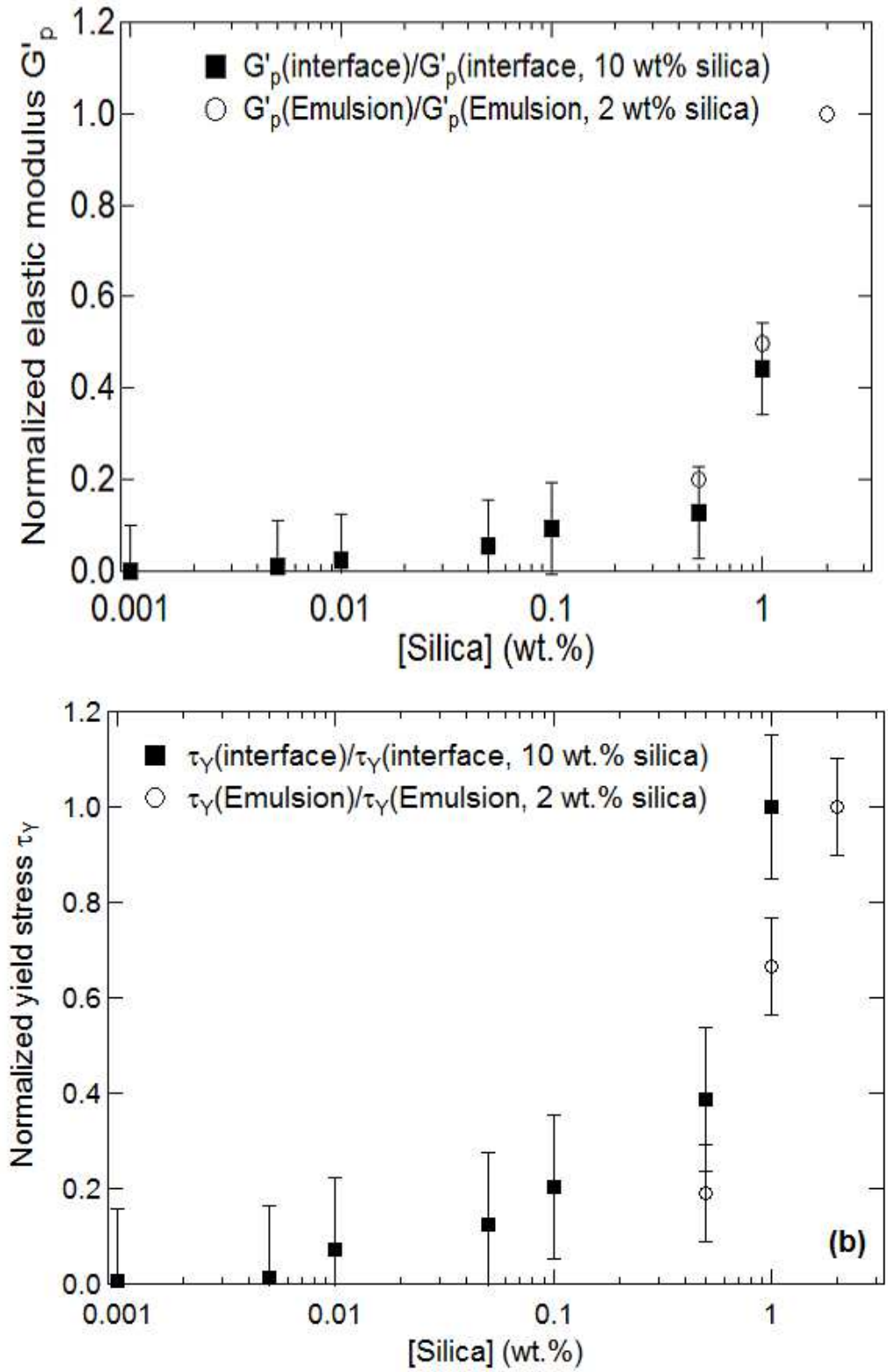

Figure 5. Parallel evolution of the (a) normalized elastic modulus at the interface and of the emulsion and (b) normalized yield stress at the interface and of the emulsion as a function of the silica content ([Silica]). The normalized elastic modulus are G_P'(interface)/G_P'(interface, 10 wt.% silica) and G_P'(Emulsion)/G_P'(Emulsion, 2 wt.% silica). The normalized yield stress are τ_Y(interface)/τ_Y(interface, 10 wt.% silica) and τ_Y(Emulsion)/τ_Y(Emulsion, 2 wt.% silica).

It seems also relevant to probe the relationship between the emulsion stability and the interfacial properties. For this purpose, the rheological properties of the emulsion were tested after 15 days of storage (Table 2 and Fig. S5 of the Supporting information, "15 days"). A slight decrease of G_P'(Emulsion) was observed for all the formulations but no macroscopic coalescence phenomenon was identified in the entire silica concentration range. To evaluate the difference in stability between the samples, the ratio of change in G_P'(Emulsion) can be used. It reads as $\frac{G_P'(0\ days)-G_P'(15days)}{G_P'(0\ days)}$. The ratios are equal to 0.20, 0.15 and 0.11 for silica content of 0.5, 1 and 2 wt.%, respectively. The ratio decreases with the silica amount. In other words, the stability of the emulsion is enhanced with the silica content. This phenomenon has been widely reported in the literature [34-36]. In parallel, recall that as the silica concentration increases, G_P'(interface) shifts to larger values. Consequently, the present results corroborate the other measurements, demonstrating that the stability of the emulsion depends significantly on the interfacial modulus [25]. A strong viscoelastic interfacial layer at the oil/water interface prevents or, at least, limits the droplets coalescence. The results confirm also that a G_P'(interface) larger than 10^{-1} N/m ensures a stability against coalescence of the droplets of the emulsion.

3.2) Effect of ionic strength

3.2.1) Interfacial rheology

The influence of the NaCl concentration on the interfacial rheological properties at the dodecane/water interface in the presence of 0.1 wt.% of silica in the oil is depicted in Fig. S6 of the Supporting information. The extracted values of the interfacial elastic modulus G_P'(interface) and yield stress (τ_Y(interface)) are displayed in the Fig. 6a,b while the yield strains (γ_Y(interface)) are given in the Table 3.

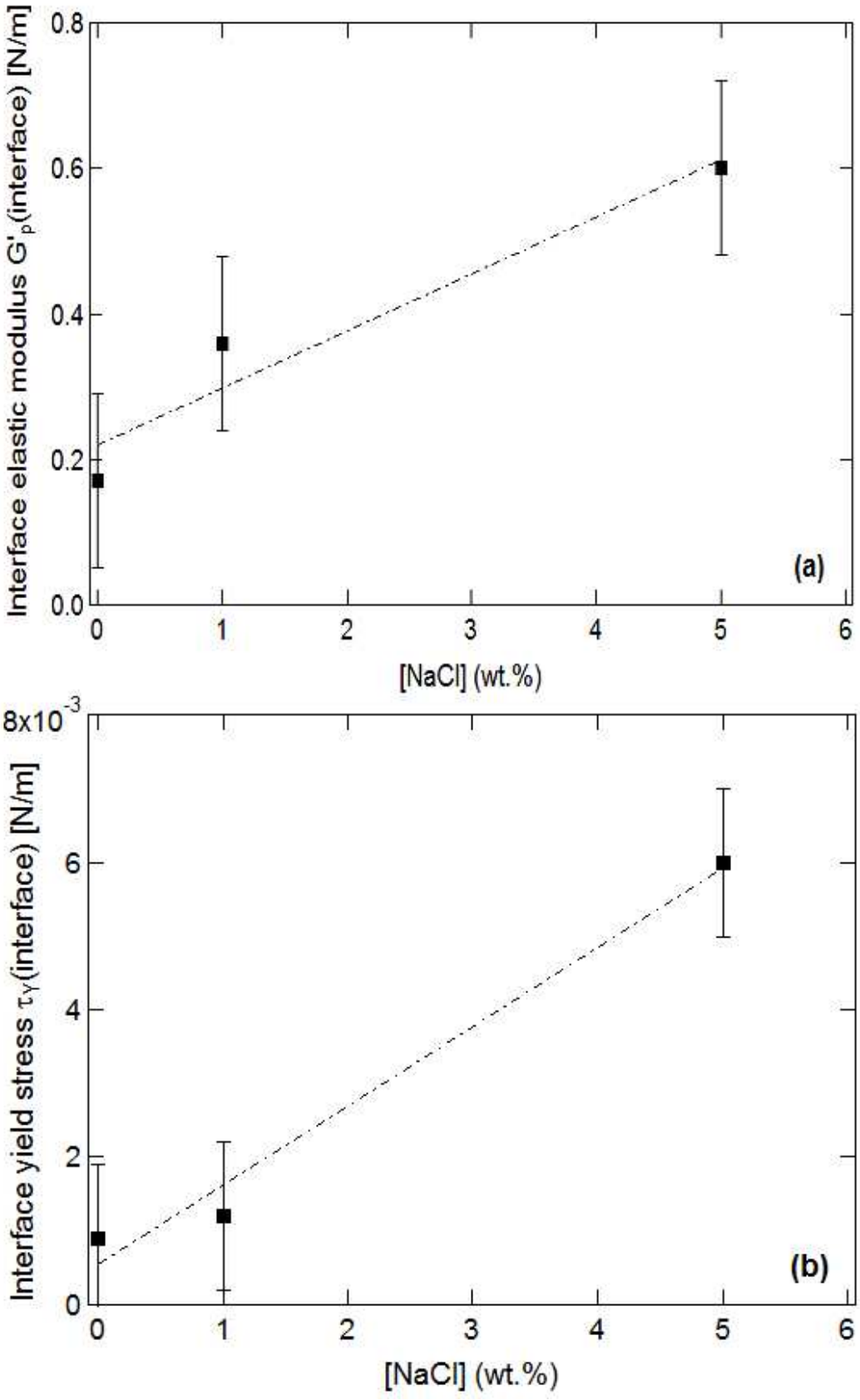

Figure 6. Evolution of the (a) interface elastic modulus $G_P{}'$(interface), and (b) interface yield stress τ_Y(interface) with the NaCl content [NaCl].

The interface elastic modulus G_P'(interface) increases with the NaCl concentration. In the presence of salt, a stronger interfacial elastic silica structure at the interface is obtained. Consequently, the salt plays a role on the rigidity of the silica film at the dodecane/water interface.

In parallel, an increase of the interfacial yield stress (τ_Y(interface)) with the salt concentration is also observed (Fig. 6b). However, the effect of the salt becomes really significant when the NaCl concentration reaches 5 wt.%. At that salt concentration, a substantial increase of τ_Y(interface) is recorded. Another interesting feature is that the evolution of the yield strain (γ_Y(interface)) with the NaCl concentrations follows the same trend (Table 3). The yield strain increases with the NaCl content but a very slight increase of γ_Y(interface) occurs in the presence of 1 wt.% of salt as compared to that in the absence of NaCl. Conversely, a significant difference can be recorded in the presence of a larger amount of salt, *i.e.* NaCl concentration of 5 wt.%. This result indicates that the extent of the interaction between the particles at the interface seems unaffected by the presence of salt when the NaCl content remains lower than or equal to 1 wt.%. The fumed silica is mainly hydrophobic due to the methylation of 70% of the hydroxyl surface groups. Actually, only 30% of the remaining SiOH surface groups of the silica can be influenced and screened by the salt. This might explain the weak effect of the NaCl content on the strength of the particle's interaction at the dodecane/water interface at this low salt content. Conversely, the particles interaction at the interface is influenced when the NaCl concentration reaches 5 wt.%. The effects of the salt on the properties of the silica, such as the interfacial viscoelastic properties, are strongly impacted by the density of charge of the silica. For highly charged silica, a small amount of salt is sufficient to produce an effect, especially on the interfacial viscoelasticity. On the opposite, when the silica bears a low density of superficial charges, a large amount of NaCl becomes necessary to produce an effect on the interfacial viscoelastic behavior. In

conclusion, the effect of salt on the interfacial viscoelastic properties is proportional to the charge density of silica. With weakly charged silica, the silica is less sensitive to the salt, hence, a large amount of NaCl is needed to obtain an effect on the viscoelasticity of the interface.

Table 3. Linear viscoelastic limits (γ_{LD}(interface) ; τ_{LD}(interface)) and threshold values (γ_Y(interface) ; τ_Y(interface)) as a function of NaCl concentration obtained from Fig. S6a-top (G'(interface) vs. shear stress $\tau \rightarrow \tau_Y$(interface) ; τ_{LD}(interface)) and Fig. S6b-bottom (G'(interface) vs. shear strain $\gamma \rightarrow \gamma_Y$(interface) ; γ_{LD}(interface)).

[NaCl] (wt.%)	$G_P{}'$(interface) [N/m]	τ_Y(interface) [N/m]	τ_{LD}(interface) [N/m]	γ_Y(interface)	γ_{LD}(interface)
0	1.7×10^{-1}	9.0×10^{-4}	3.9×10^{-4}	1.7×10^{-2}	2.2×10^{-3}
1	3.6×10^{-1}	1.2×10^{-3}	7.9×10^{-4}	1.9×10^{-2}	2.4×10^{-3}
5	6.0×10^{-1}	6.0×10^{-3}	5.0×10^{-3}	6.0×10^{-2}	1.1×10^{-2}

3.2.2) Emulsion rheology

In the presence of NaCl, reverse W/O Pickering emulsions were prepared. The silica content was fixed to 1 wt.%. All the emulsions could be diluted in dodecane and displayed conductivities lower than 10^{-5} S cm^{-1}. Fig. S7 of the Supporting information highlights the effect of the electrolyte concentration on the droplet size distribution. The electrolyte concentration has a relatively weak impact on the droplet size distribution. The droplet sizes do not substantially vary with the electrolyte concentration with droplet size ranging from 10 to 60 µm. The calculated mean droplet size of the emulsions are equal to 23 µm, 26 µm, and 25 µm for emulsions prepared with 0, 1 and 5 wt.% of NaCl, respectively.

The whole results of the oscillatory tests (elastic modulus of reverse Pickering emulsions against shear strain and shear stress for various NaCl electrolyte concentrations) are provided in the Fig. S8 of the Supporting information. The impact of NaCl electrolyte concentration on

the storage modulus is presented in Fig. 7a. The corresponding linearity limits in terms of yield stress τ_Y(Emulsion) and yield strain γ_Y(Emulsion) are displayed in Fig. 7b and Table 4.

The G_P'(Emulsion) increases as the NaCl concentration is enhanced. As a matter of fact, a weak variation in G_P'(Emulsion) takes place when the NaCl content shifts from 0 wt.% to 1 wt.% since G_P'(Emulsion) are equal to 1232 Pa and 1273 Pa, respectively. Then, the increase of the amount of NaCl from 1 wt.% to 5 wt.%, produces a significant change in the emulsion elastic modulus (from 1273 Pa to 1688 Pa). Similarly, the yield stress slightly increases from 0 wt.% to 1 wt.% NaCl. Then, a greater increase of emulsion viscoelasticity at 5 wt.% NaCl is reported through a higher value of τ_Y(Emulsion).

Additionally, since yield strains do not present a broad difference between samples at 0 and 1 wt.% of salt, no change in the extent of droplet interactions is identified in that range of NaCl concentrations. Conversely, when the salt concentration reaches 5 wt.%, the extent of interaction between the droplets is modified.

Table 4. Linear viscoelastic limits (γ_{LD}(Emulsion) ; τ_{LD}(Emulsion)) and threshold values (γ_Y(Emulsion) ; τ_Y(Emulsion)) as a function of electrolyte concentration obtained from Fig.S8-top (*G'*(Emulsion) vs. shear strain $\gamma \rightarrow \gamma_Y$(Emulsion) ; γ_{LD}(Emulsion)) and Fig. S8-bottom (*G'*(Emulsion) vs. shear stress $\tau \rightarrow \tau_Y$(Emulsion) ; τ_{LD}(Emulsion)).

[NaCl] (wt.%)	G_P'(Emulsion) [Pa]	τ_Y(Emulsion) [Pa]	τ_{LD}(Emulsion) [Pa]	γ_Y(Emulsion)	γ_{LD}(Emulsion)
0	1232	74	12	0.049	0.0127
1	1273	84	12	0.045	0.0127
5	1688	133	17	0.060	0.0372

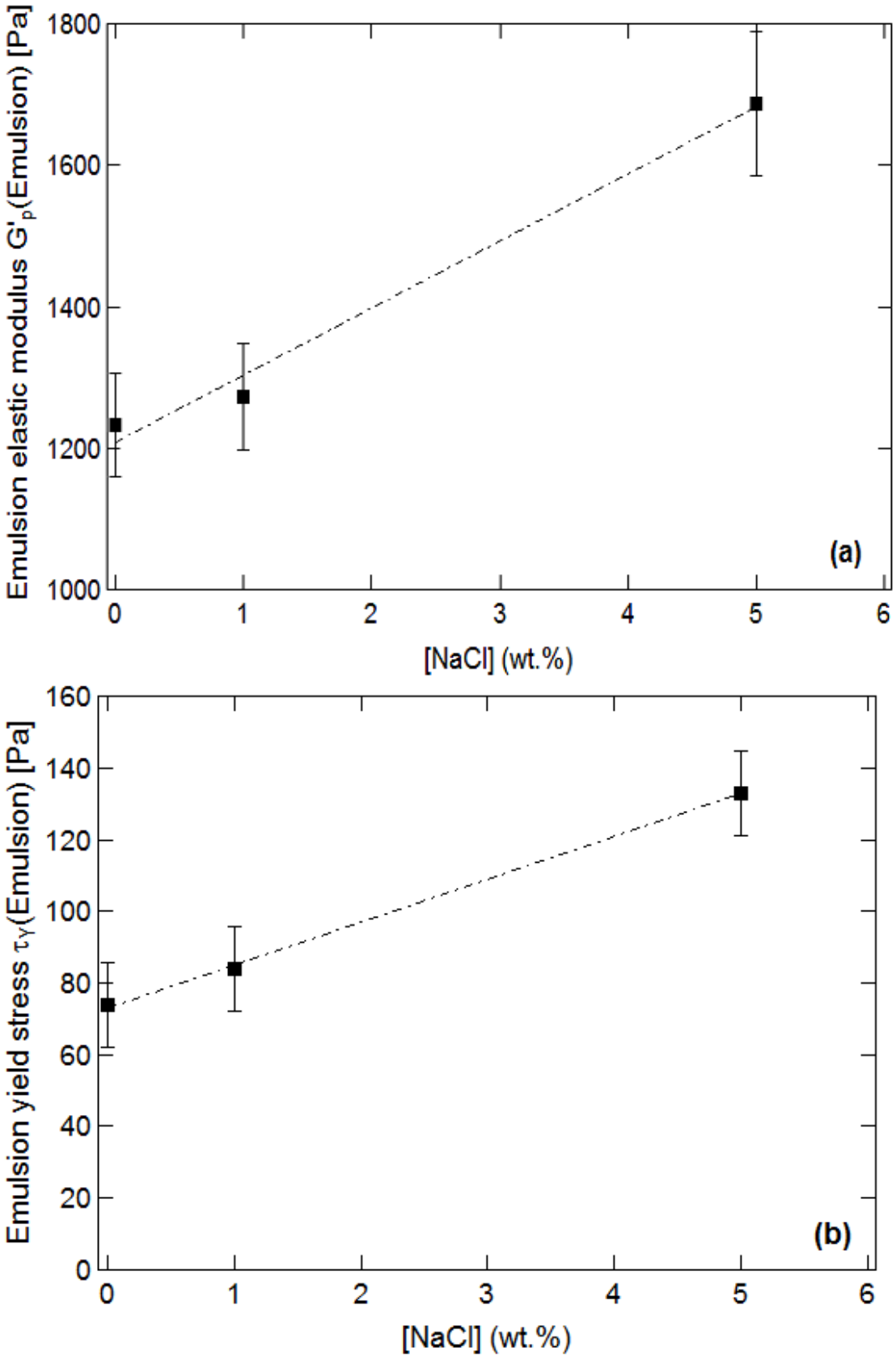

Figure 7. Evolution of the (a) emulsion elastic modulus G_P'(Emulsion), and (b) emulsion yield stress τ_Y(Emulsion) with the NaCl concentration. [Silica] = 1 wt.%.

3.2.3) Interfacial vs bulk rheology

As previously described with the silica content, the rheological properties of the bulk and at the interface follow similar evolution. The $G_P{}'$ of the emulsion and the interface are likely to evolve in a similar manner. The two moduli increase by increasing the NaCl concentration. The yield strain and yield stress at the interface and in the bulk exhibit comparable evolutions.

To emphasise the similarities between the interfacial and volumetric phenomena, $G_P'(\text{Emulsion})$ were plotted against $G_P'(\text{interface})$ for each NaCl concentration. The results are given in Fig. 8a. Obviously, each point corresponds to the same formulation with similar NaCl concentration. The $G_P'(\text{Emulsion})$ increases with the $G_P'(\text{interface})$. This indicates that the enhancement of the elastic modulus at the interface induces an improvement of the elastic modulus in the bulk of the emulsion. The rigidification of the silica film at the interface produces an increase of the elasticity of the emulsion. Although this behaviour was expected, this is the first time that it is reported in the scientific literature.

It is also relevant to compare the yield stress at the interface and for the emulsion by plotting τ_Y(Emulsion) vs τ_Y(interface). The results are displayed in Fig. 8b. An increase of the τ_Y(Emulsion) with τ_Y(interface) is observed. This means that the corresponding yield stress of the emulsion can be linked to the yield stress of the interface. This is the first time that this kind of correlation between volume and interface properties of emulsions is reported.

Consequently, all these results confirm the fact that all that impacts the viscoelastic properties at the interface produces a change of the volume viscoelasticity of the emulsion.

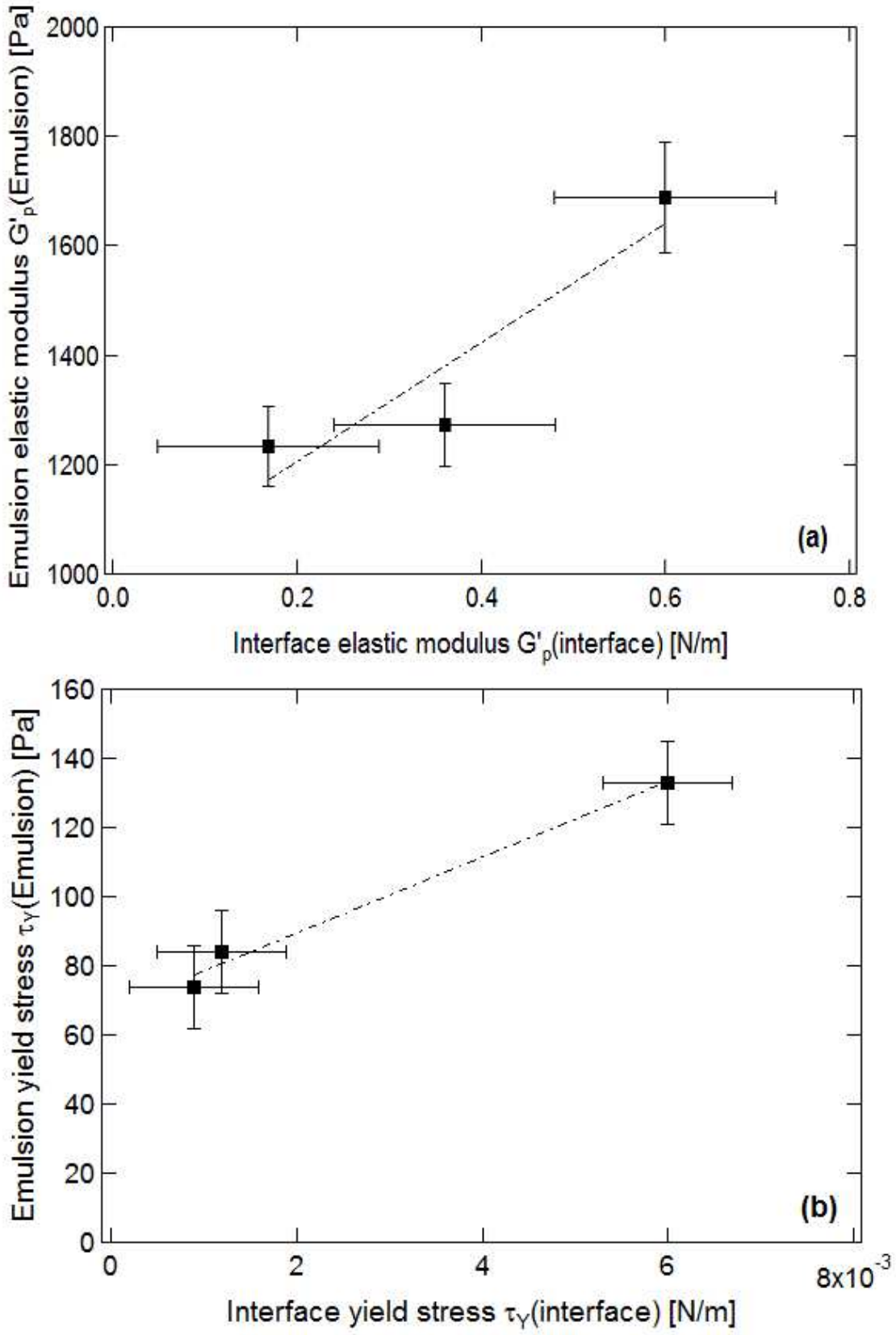

Figure 8. Relationship between the interfacial and volumetric rheological properties. (a) Evolution of the emulsion elastic modulus $G_P{}'$(Emulsion) as a function of the interface elastic modulus G_P'(interface). (b) Evolution of the emulsion yield stress τ_Y(Emulsion) with the interface yield stress τ_Y(interface).

4) Conclusion

The objective of this article was to explore the relationship between interfacial and bulk emulsion viscoelasticity. To this aim, semi-concentrated reverse W/O (water-in-dodecane) Pickering emulsions containing a dispersed phase volume fraction of 0.66 were considered. Partially hydrophobic silica particles were used as dispersing agent while the emulsification was produced by an Ultra-Turrax® homogenizer. Interfacial and bulk viscoelastic properties were addressed *via* oscillatory shear rheology experiments. Various formulation parameters, including the silica and NaCl concentrations, were investigated.

The interfacial and emulsion viscoelasticity were affected by the formulation parameters. On the one hand, a relationship between the emulsion and interfacial viscoelasticity properties was obtained when varying the silica content. The elastic modulus G_P' increased with the silica content both for the emulsion and at the interface. Power law dependencies towards the silica content were recorded for the interface and the emulsion elastic modulus. Similarly, the increase of the silica content lead to an enhancement of the yield stress τ at the interface and for the emulsion. The normalized G_P'(interface) and G_P'(Emulsion) evolved in a similar manner as a function of the silica uptake. In particular, the change of normalized elastic modulus from 0.5 to 1 wt.%. was similar for both systems. These conclusions applied also for the normalized yield stresses. The increase of the silica content induced a rigidification of the dodecane/water interface (as G_P'(interface) and τ_Y(interface) increased) which produced a rigidification of the emulsion and droplets (increase of G_P'(Emulsion) and τ_Y(Emulsion)). On the other hand, when increasing the NaCl concentration, the silica film at the interface became stronger (increase of G_P'(interface) and τ_Y(interface)) and the viscoelastic properties of the emulsion were enhanced (increase of G_P'(Emulsion) and τ_Y(Emulsion)). Relationships between the viscoelastic properties at the interface and for the emulsion were highlighted

when $G'_P(\text{Emulsion})$ were plotted against $G'_P(\text{interface})$ and $\tau_Y(\text{Emulsion})$ versus $\tau_Y(\text{interface})$ for each NaCl concentration.

To conclude, this work suggests that all that impacts the viscoelastic properties at the interface (silica content and NaCl concentration) leads to a change of the viscoelasticity of the emulsion. The present results provide first guidelines to obtain a quantitative relationship between interfacial and emulsion viscoelasticity. Additional data are necessary to establish mathematical relationships. Future work will also address the validation of the methodology with lower and larger dispersed volume fractions, other Pickering emulsions such as oil-in-water emulsions and other particles including soft and hard particles. The strong relationship between the interfacial phenomena and the emulsion properties highlights that the interfacial rheology can be used as an indirect measurement of the emulsification capacity for cosmetic applications. The interfacial rheology data can be employed to test the feasibility of emulsifications based on the screening of series of oils and particles with the aim to find the optimal stabilizing agents for a given oil.

References

[1] V. Schmitt, M. Destribats, R. Backov, Colloidal particles as liquid dispersion stabilizer: Pickering emulsions and materials thereof, C. R. Physique 15 (2014) 761-774.

[2] Y. Chevalier, M.A. Bolzinger, Emulsions stabilized with solid nanoparticles: Pickering emulsions, Colloids Surf. A 439 (2013) 23-34.

[3] J. Wu, G-H Ma, Recent studies of Pickering emulsions: Particles make the difference, Small 12 (2016) 4633–4648.

[4] Y. Yang, Z. Fang, X. Chen, W. Zhang, Y. Xie, Y. Chen, Z. Liu, W. Yuan, An overview of Pickering emulsions: Solid-particle materials, classification, morphology, and applications, Front. Pharmacol. 8 (2017) 287.

[5] C. Albert, M. Beladjine, N. Tsapis, E. Fattal, F. Agnely, N. Huang, Pickering emulsions: Preparation processes, key parameters governing their properties and potential for pharmaceutical applications, J. Control. Release 309 (2019) 302-332.

[6] M. Destribats, S. Gineste, E. Laurichesse, H. Tanner, F. Leal-Calderon, V. Héroguez, V. Schmitt, Pickering emulsions: What are the main parameters determining the emulsion type and interfacial properties? Langmuir 30 (2014) 9313–9326.

[7] S.F. Velandia, P. Marchal, C. Lemaitre, V. Sadtler, T. Roques-Carmes, Evaluation of the repartition of the particles in Pickering emulsions in relation with their rheological properties, J. Colloid Interface Sci. 589 (2021) 286-297.

[8] M. Dinkgreve, K. P. Velikov, D. Bonn, Stability of LAPONITE®-stabilized high internal phase Pickering emulsions under shear. Phys. Chem. Chem. Phys. 18 (2016) 22973-22977.

[9] A.J. Mendoza, E. Guzman, F. Martinez-Pedrero, H. Ritacco, R.G. Rubio, F. Ortega, V.M. Starov, R. Miller, Particle laden fluid interfaces: Dynamics and interfacial rheology, Adv. Colloid Interface Sci. 206 (2014) 303-319.

[10] O.S. Deshmukh, D. van den Ende, M. Cohen Stuart, F. Mugele, M.H.C. Duits, Hard and soft colloids at fluid interfaces: Adsorption, interactions, assembly & rheology, Adv. Colloid Interface Sci. 222 (2015) 215-227.

[11] N. Jaensson, J. Vermant, Tensiometry and rheology of complex interfaces, Curr. Opin. Colloid Interface Sci. 37 (2018) 136-150.

[12] L.M.C. Sagis, P. Fischer, Nonlinear rheology of complex fluid-fluid interfaces, Curr. Opin. Colloid Interface Sci. 19 (2014) 520-529.

[13] D. Pradilla, S. Simon, J. Sjoblom, J. Samaniuk, M. Skrzypiec, J. Vermant, Sorption and

interfacial rheology study of model asphaltene compounds, Langmuir 32 (2016) 2900-2911.

[14] W. Marczak, M. Rogalski, A. Modarressi, E. Rogalska, A model of compression isotherms for analyzing particle layers, Colloids Surf. A 489 (2016) 128-135.

[15] Y. Gong, Z. Zhang, J. He, Deformation and stability of core−shell microgels at oil/water interface, Ind. Eng. Chem. Res. 56 (2017) 14793-14798.

[16] J. Kragel, S.R. Derkatch, Interfacial shear rheology, Curr. Opin. Colloid Interface Sci. 15 (2010) 246-255.

[17] C.O. Klein, A. Theodoratou, P.A. Ruhs, U. Jonas, B. Loppinet, M. Wilhelm, P. Fischer, J. Vermant, D. Vlassopoulos, Interfacial Fourier transform shear rheometry of complex fluid interfaces, Rheol. Acta 58 (2019) 29-45.

[18] K. Golemanov, S. Tcholakova, N. Denkov, E. Pelan, S.D. Stoyanov, Surface shear rheology of saponin adsorption layers, Langmuir 28 (2012) 12071-12084.

[19] J.S. Hong, P. Fischer, Bulk and interfacial rheology of emulsions stabilized with clay particles, Colloids Surf. A 508 (2016) 316-326.

[20] E. Santini, L. Liggieri, L. Sacca, D. Clausse, F. Ravera, Interfacial rheology of Span 80 adsorbed layers at paraffin oil-water interface and correlation with the corresponding emulsion properties, Colloids Surf. A 309 (2007) 270-279.

[21] D. Langevin, Influence of interfacial rheology on foam and emulsion properties, Adv. Colloid Interface Sci. 88 (2000) 209-222.

[22] H.W. Yarranton, D.M. Sztukowski, P. Urrutia, Effect of interfacial rheology on model emulsion coalescence. I. Interfacial rheology, J. Colloid Interface Sci. 310 (2007) 246-252.

[23] M.B.J. Meinders, T. van Vliet, The role of interfacial rheological properties on Ostwald ripening in emulsions, Adv. Colloid Interface Sci. 108 (2004) 119-126.

[24] G. Dockx, S. Geisel, D.G. Moore, E. Koos, A.R. Studart, J. Vermant, Designer liquid-liquid interfaces made from transient double emulsions. Nat. commun. 9 (2018) 1-8.

[25] M. Kamkar, P. Bazazi, A. Kannan, V.C. Suja, S.H. Hejazi, G.G. Fuller, U. Sundararaj, Polymeric-nanofluids stabilized emulsions: Interfacial versus bulk rheology, J. Colloid Interface Sci. 576 (2020) 252-263.

[26] D. Pradilla, A. Barrera, M. G. Sætran, G. Sørland, O. Alvarez, Mechanisms of physical stabilization of concentrated water-in-oil emulsions probed by pulse field gradient nuclear magnetic resonance and rheology through a multiscale approach. Langmuir 34 (2018) 9489-9499.

[27] M. Dinkgreve, J. Paredes, M.M. Denn, D. Bonn, On different ways of measuring "the" yield stress. J. NonNewton. Fluid Mech. 238 (2016) 233-241.

[28] S. Reynaert, P. Moldenaers, J. Vermant, Interfacial rheology of stable and weakly aggregated two-dimensional suspensions, Phys. Chem. Chem. Phys. 9 (2007) 6463–6475.

[29] Y.-J. Lin, S. Barman, P. He, Z. Zhang, G.F. Christopher, S.L. Biswai, Combined interfacial shear rheology and microstructure visualization of asphaltenes at air-water and oil-water interfaces, J. Rheol. 62 (2018) 1-10.

[30] W.H. Shih, W.Y.S. Seong-Il Kim, J. Liu, A. Aksay, Scaling behavior of the elastic properties of colloidal gels, Phys. Rev. A 42 (1990) 4772-4779.

[31] M.V. Mironova, S.O. Ilyin, Effect of silica and clay minerals on rheology of heavy crude oil emulsions, Fuel 232 (2018) 290-298.

[32] L. Hohl, S. Röhl, D. Stehl, R. Klitzing, M. von Kraume, Influence of nanoparticles and drop size distributions on the rheology of w/o Pickering emulsions, Chem. Ing. Tech. 88 (2016) 1815–1826.

[33] V. Trappe, V. Prasad, L. Cipelletti, P.N. Segre, D.A. Weitz, Jamming phase diagram for attractive particles, Nature 411 (2001) 772-775.

[34] S. Arditty, C.P. Whitby, B.P. Binks, V. Schmitt, F. Leal-Calderon, Some general features of limited coalescence in solid-stabilized emulsions, Eur. Phys. J. E. 11 (2003) 273-281.

[35] B.P. Binks, J. Philip, J.A. Rodrigues, Inversion of silica-stabilized emulsions induced by particles concentration, Langmuir 21 (2005) 3296-3302.

[36] E. Tsabet, L. Fradette, Effect of the properties of oil, particles, and water on the production of Pickering emulsions, Chem. Eng. Res. Des. 97 (2015) 9-17.